

# 2005 Best Paper - Quantification of Melting Progression During Twin Screw Extrusion Using the Pulse Perturbation Technique Part I

[Print](#)

[\(10\)](#) » [2006 Best Paper 1 - Numerical and Experimental Study of Dispersive Mixing of Agglomerates](#) » [2006 Best Paper 2 - Using Extreme Barrel Diameters to Verify the Numerical Simulation of Single-Screw Extruders](#) » [2005 Best Paper - Quantification of Melting Progression During Twin Screw Extrusion Using the Pulse Perturbation Technique Part I](#)

## Quantification of Melting Progression During Twin Screw Extrusion Using the Pulse Perturbation Technique Part I: Method, Experiment and New Insights

Mark D. Wetzal, Donald A. Denelsbeck, Susan L. Latimer - E. I. du Pont de Nemours and Co., Inc., Wilmington, Delaware, 19880  
Chi-Kai Shih - Chi-Kai Shih, L.L.C., Wilmington, Delaware

### Abstract

Steady state and pulse perturbation monitoring of the melting process in a twin-screw extruder has been carried out. While steady state measurements quantify the total mechanical energy input, they provide no information about the melting progression in the working section. Previously [2], Polypropylene and Polystyrene data were presented for several operating conditions. In this paper, the behaviors of four different resins are examined in more detail. Quantification of melting time and intensity using pulse perturbation power and RTD responses has been attempted. The effects of operating conditions and simple changes in screw design are examined. Multivariate statistical analysis using Principal Components Analysis of independent operating variables, monitored and derived parameters is described.

### Introduction

No kinetic information can be derived from steady state monitoring of extrusion. A novel flow perturbation method, the "Pulse Technique" was introduced [1-3] to quantify the dynamic behavior of melting and chemical reactions in twin-screw compounding. Certain fundamental details during the extrusion of semi-crystalline and amorphous polymers, such as Polypropylene (PP), Polystyrene (PS), or PP/PS polymer blends were described with respect to the kinetics of melting and energy input. The effects of extrusion conditions, such as throughput/screw speed (Q/N) ratio, were examined. A specialized, high-speed data acquisition system, the "Extrusion Pulse Analysis System" (EPAS) was employed to enable on-line monitoring and data analysis of the extruder's response to an imposed mass disturbance to provide a real-time diagnosis of polymer processes in laboratory and manufacturing applications [1, 2].

The pulse technique opens the possibility to define the kinetics as well as the physics of melting during extrusion in more detail. Parts I and II [4] describe advances made in test and analytical methods, and new insights gained from the interpretation of the steady state, pulse power and residence time distribution (RTD) responses relating to the underlying physics. In Part I, four different resins were used over a variety of operating conditions (Q, N, barrel temperature) and screw geometries. The effect of material form (pellet and powder) was examined.

In this paper, the melting sequence previously defined [1,5-6] is decomposed into two flow regimes; 1) a plug flow state that includes solid conveying, compaction/frictional heating (FED) at the start of the filled melting zone and bulk plastic deformation (PED), transitioning to 2) fluid flow with lubrication by a melt phase (transitional flow) and viscous energy dissipation (VED) in a liquid phase suspension with un-melted solids. Refined test methods were developed to identify and separate each melting stage. By comparing several polymer systems, material property effects in plug and fluid flow regions can be captured. Using similar polymers with different molecular weights allows the fluid flow mode to be probed.

New analytical methods were developed where the pulse specific energy input in time is decomposed into the plug and fluid flow regimes providing new engineering parameters that may be useful in product and process development or troubleshooting. Pulse and RTD responses were compared with steady state power consumption, with an examination of energy loss. Steady state and dynamic variables were combined and examined statistically using a multivariate method, Principal Components Analysis (PCA) [7]. The pulse mass, a momentary increase of 100% to 500% of the steady state throughput, causes a significant perturbation of solid and fluid flows, requiring careful interpretation of the time signals relative to the steady state melting progression down the length of the screw.

### Experiment

Experiments were conducted on a Coperion W&P ZSK-30mm intermeshing, co-rotating twin-screw extruder. In previous experiments [1], the "8-0" transition section added a second filled region consuming mechanical energy. Fig. 1 shows the open-discharge configuration used in this work with screw #1 and probe locations. The other screws (2 and 3) are also shown in Fig. 1. With this setup, the motor power included only the melting zone and drive system losses. However, reliable polymer melt temperatures could not be obtained. Semi-crystalline and amorphous polymers used were:

- 1) Polypropylene (PP) - Atofina 3480Z, 4.8 MFR
- 2) Polystyrene (PS) - Dow Styron® 666D, 8 MFR

- 3) Polyethylene (PE) - Alathon® M6060 (6 MI) and H6018 (18 MI)  
 4) Polypropylene Powder - Atofina 3480Z, 4.8 MFR

Solid material properties are listed in Table 1. Thermal properties, including enthalpies from DSC scans and melt viscosities at 200°C and shear rates at screw speed of 200RPM are shown in Table 2.

PP and PE pulse masses were fixed at 6.5gm while PS used 8.5 gm to increase signal to noise ratio with 0.5gm of a 20% by weight TiO<sub>2</sub> concentrate added as the RTD tracer. The “Extrusion Pulse Analysis System” (EPAS) [1,2] was used to record the measurements. An optical RTD probe was mounted at the end of the melting zone over the last reverse-pumping element [1]. Data were scanned at 60Hz, decimated to 20Hz and filtered with low-pass FIR and 3-tap median filters. Pulse tests were replicated 8 times and averaged to reduce variability as shown in Fig 2. Steady state, RTD and pulse response variables are tabulated in Part II [4].

## Discussion of Results

### Pulse Response: Kinetics of Melting and Flow Regimes

Fig. 2 shows the pulse power and RTD responses for PP at 9.1hg/hr and 200RPM. The pulse power was normalized by the pulse mass and the steady state power by the throughput. PP and PS results were consistent with previous tests demonstrating reproducibility [1]. The pulse specific energy input was obtained by removing the power signal steady state baseline with a linear technique then integrating the power change from time 0. At 9.1kg/hr and 200RPM, PP and PS specific energies were 400 and 220J/g in [1] and 389 and 244J/g in this test. From Fig. 2, a transport delay,  $t_{xport}$ , of 4.4s was measured with no additional energy input followed by a sharp rise in power, peaking at 5.9s,  $t_{Peak}$ , then decaying to the baseline within 15 to 20s.

It is proposed that the dynamic response is due to the additional energy dissipation of the pulse material under- going the following sequence of flow regimes; I) solid conveying with little power consumption, II) a rapid rise in power from to friction (FED) followed by deformation (PED) of the solid flowing as a plug, III) near the peak the rapid change in power from material softening and the onset of melting leading to lubrication (transition), and IV) the decay of the power due to continued melting as the solid plug becomes a slurry with fluid flow and viscous energy dissipation (VED). For analysis, the pulse power profile was separated into the plug and fluid flow segments as shown in Fig 2, corresponding to energy dis- sipation before and after the onset of melting.

Fig 3 shows the pulse power response with the baseline removed, and by integration, the specific energy input ( $SpE_{Pulse}$ ) for four materials, PP, PS, PE MI6 and PE MI18. The power response for all materials followed the same profile as described for PP. Melting was initiated earlier for PS, while PP and PE differed only in peak height. Table 3 lists the steady state, RTD and extracted pulse response variables. The pulse plug flow energy input ( $SpE_{Plug}$ ) accounted for 30-40% of the total while 60-70% was in the fluid flow regime ( $SpE_{Fluid}$ ). Fig 4 shows  $SpE_{Plug}$  and  $SpE_{Fluid}$  plotted against the enthalpy required to reach the onset of melting and to complete the phase transition. For PP and PE, the plug flow energy was insufficient to initiate melting, while the energy input for PS matched the enthalpy to reach Tg. For PP and PS, the fluid flow region provided an excess of energy to complete melting, but only enough energy was input for PE to reach the melting point.  $SpE_{Pulse}$  followed the same trend as the material enthalpies, indicating that the pulse response is sensitive to thermal properties. For PS,  $SpE_{Plug}$  was equivalent to the energy required to induce the phase transition. The early peak and rapid decay are consistent with compressive stress-strain properties as a function of temperature governing the PED mode [5]. In Fig 3, PS and PP power peak heights were similar, but PS entered the transition state earlier, since PS reached a softened, or rubbery state at a lower temperature than PP [5]. Since PE is a low-modulus, more deformable material, the peak height was the lowest. This suggests that the pulse curve before or up to the peak captures solid stress-strain properties for PED. PP and PE power pro- files were almost identical in time, suggesting that the melting sequence and transitions are similar and occur at the same axial locations. PE MI18 (low MW) had a slightly higher power peak and  $SpE_{Pulse}$  than PE MI6 (high MW). This trend is consistent with the thermal properties, where the PE MI18 enthalpy requirement is greater, indicating perhaps a higher degree of crystallinity.

For all materials as listed in Table 3, the steady state energy input ( $SpE_{StState}$ ) exceeded the enthalpy to reach the 200°C barrel temperature and was always greater than  $SpE_{Pulse}$ . The measured power includes losses from the motor and transmission, but drive system efficiency alone does not account for the magnitude of the difference. It is proposed that the pulse perturbation affects the melting process primarily in the channel while the energy dissipated in the clearances remains essentially constant. Power consumption may be expressed as

$$P_{Total} = P_{Channel} + (P_{Clearance} + P_{Drive}) \quad (1)$$

where the “loss” term includes VED in the clearances and drive system efficiency effects. From Fig 4,  $SpE_{Plug}$  changed little with material type, while  $SpE_{Fluid}$  trended with enthalpy data, with the exception of the magnitude in PE relative to PP.  $SpE_{StState}$  for MI18 was less than MI6, indicating that the viscosity and dissipation in the clear- ances and heat transfer with the barrel played an important role in melting energy input. Energy input and loss are discussed in more detail in Part II [4].

Fig 5 suggests that the initial rise of the pulse power curves have a shape consistent with drag-induced flow of a plug in single screw extrusion [11]. In the plug flow of a screw pump, pressure is an exponential function of ge- ometry, operating conditions and material friction coeffi- cients, and energy dissipation is proportional to pressure. In the twin-screw extruder, the screws are non-rectangular in shape, the deformable plug travels through the nip re- gion, and the frictional energy is generated at the barrel, screws and pellet-to-pellet surfaces [6]. These effects may contribute to the deviation from the ideal exponential function. For the FED mode, the plug flow assumption used in the pulse analysis seems reasonable. In the PS system, the early power rise may be attributed to a greater coefficient of friction and a pellet shape that increased channel fill due to a lower volume fraction of polymer as listed in Table 1.

An analytical method was developed to quantify the rate of temperature rise during melting using the  $SpEPulse$  curve and material enthalpy data. By assuming plug flow and adiabatic conditions, a temperature profile was calcu- lated as shown in Fig 6. The final adiabatic temperature estimates, TAD, are listed in Table 3. PS reached Tg by  $t_{Peak}$  and the melt flow state well before PP and PE ap- proached their melting points. PP and PS final values were 20 and 30°C above measured melt temperatures, indicating that heat transfer played a significant role in melting, especially in the VED stage. While the plug flow assumption is not valid in the fluid flow regime, since there was significant spreading as measured by the RTD, this analysis does show relative rates of temperature rise linked to material specific heat capacity.

# Effect of Molecular Weight and Melt Viscosity

A test method was developed to quantify the effects of molecular weight and viscosity on melting kinetics. During high-viscosity PE MI6 and low-viscosity PE MI18 extrusions, MI6 and MI18 pulses were introduced. Fig 7 shows the power responses where the plug flow regimes (PED and FED) were identical, but there was a pulse material-specific grouping at the peak. The high-viscosity MI6 pulses had a power peak less than the MI18 material. This may be due to a slightly lower modulus in the MI6 material reducing the PED. By pulsing the MI18 extrusion with MI6 material (MI18/MI6), the high-viscosity-rich blend dissipated more energy in the fluid flow regime and the power curve deviated from the MI18/MI18 profile at 6.7s. Similarly the MI6/MI18 power dipped below MI6/MI6 with reduced viscous dissipation at 7.2s. This indicates that these pulse power curves may be used to separate the transition state from the VED melting mode.

# Effect of Barrel Temperature and Heat Transfer

Heat transfer effects during melting as measured by the pulse technique were reproduced [1]. Fig 8 plots  $SpE_{StState}$ ,  $SpE_{Pulse}$ ,  $SpE_{Plug}$  and  $SpE_{Fluid}$  against barrel temperature, TBBL, with linear fits. For PP,  $SpE_{StState}$  and  $SpE_{Pulse}$  slopes were the same with an offset of 253J/g.  $SpE_{Plug}$  and  $SpE_{Fluid}$  also decreased with increasing TBBL, indicating FED, PED, lubrication and VED modes were all influenced by heat transfer. In the PS system,  $SpE_{StState}$  and  $SpE_{Pulse}$  slopes were the same and  $SpE_{Fluid}$  decreased with increasing TBBL.  $SpE_{Plug}$  changed very little, indicating that the FED and PED were not affected, since the transition was very fast. The rate of energy input change was estimated to be -2.3J/gm/C for PP and -2.9J/gm/C for PS. The RTD and NDM did not change, indicating that the melting sequences and transitions were similar.

# Effect of Material Form: Powder and Pellets

A test was conducted to determine if the pulse technique could quantify the effect of material form on melting. A PP powder extrusion was pulsed with 6.5gm of powder with tracer. Fig 9 shows the power responses for pellet and powder extrusions at 9.1kg/hr and 200RPM. For the powder, there was a slight lag in  $t_{Delay}$  but  $t_{Peak}$  was delayed significantly. The rate of increase in power in the FED region was less than the pellet extrusion. Pellets can form a randomly packed plug very quickly, while powder compression takes more time and screw length causing the pressure to rise more slowly. Consequently, the powder system may enter a PED state later with less deformation before transitioning to the lubrication mode. Unexpectedly, more pulse energy was dissipated in the VED mode, with  $SpE_{Powder}$  430J/g and  $SpE_{Pellet}$  390J/g. Further investigation is needed in this area.

# Multivariate Statistical Analysis

Principal Components Analysis (PCA) [7] was applied to evaluate the utility of this linear, multivariate statistical approach using pulse, RTD and steady state data for Q/N and TBBL states in PP and PS systems. A 14 state (scores) by 19 variables (loads) matrix was used with data normalized to zero mean and unit standard deviation. Fig 10 shows a contribution plot where four principal components (PC's) captured 90% of the variance ( $\sigma^2$ ) in the data set. PC and PC captured 56% and 24% of  $\sigma^2$  due to Q 12 and N changes. PC captured 10% of  $\sigma^2$  attributed to 3 TBBL. Most variables, especially RTD, pulse times and NDM were controlled by Q and N. Several steady state variables reflected the influence of TBBL as did  $SpE_{Pulse}$ . As previously noted, the melt temperature measurement was poor, confirmed with 80% of  $\sigma^2$  captured. An unexpected result was that the pulse power peak had poor correlation (75%  $\sigma^2$ ), while the peak time captured 95%  $\sigma^2$ .

Fig 11 shows a PCA for PS as a function of Q, N and TBBL. Three PC's captured 95% of  $\sigma^2$ . While the linear model structure was different from the PP system, the relative effects of the independent variables similar to PP with few exceptions. PC1 indicated that the pulse peak was a strong function of Q and N. For PS, TBBL was more significant than for PP and had a stronger effect on other variables, including  $SpE_{Pulse}$  and NDM.

# Effect of Screw Design

Three screw designs shown in Fig 1 were tested with a PP extrusion. Small changes were made to the downstream configuration. In screw 2, the last reverse pumping element was removed. For screw 3, the last forward kneading block (KBR) of screw 2 was replaced with a neutral kneading block (KBN). Table 4 lists measurements and Fig 12 shows the pulse power and RTD responses at 9.1kg/hr and 200RPM. Small differences were measured in the steady state power, pulse power and  $SpE_{Pulse}$ . This indicates that FED and PED melting modes were not altered appreciably. There were significant changes to the RTD, especially in the spread as measured with  $t_{Width}$ . While the pulse response did detect changes in the VED melting stage, it may not be sensitive enough to measure small differences in the melt flow regime with a low concentration of un-melted solids. The pulse mass spreading as recorded by the RTD may minimize the mass flow effect near the end of the melting zone where the additional energy dissipation decays close to the noise level.

A PCA was run with 6 Q/N states run for each screw. The contributions plot in Fig 13 shows that PC2 and PC4 captured the screw design effects, representing 26% of  $\sigma^2$ . Pulse variables, such as NDM,  $SpE_{Plug}$  and  $SpE_{Fluid}$  all correlated with screw design.

# Conclusions

The pulse perturbation method was enhanced to probe melting in a twin-screw extruder in more detail. The power response was used to split the energy input into a plug flow regime involving solid conveying, frictional and deformational dissipation, and a fluid flow regime including the onset of melting, lubrication, two-phase flow with viscous dissipation with significant spreading as measured with RTD sensors. The plug flow mode had short residence time and consumed about 30- 40% of the total mechanical energy input for PP and PE and 40-50% for PS.

A new experimental method was developed to quantify the effects of molecular weight on melting. By extruding and pulsing with high and low-viscosity PE, the plug flow regime was found to change little with the exception of the pulse power peak height. In the fluid flow region, the transition to and extent of VED melting was identified. Pulse tests showed how barrel temperature and heat transfer play a significant role in melting in both plug and fluid flow regimes. Pulse and steady state specific energy input followed similar linear trends, but with different offsets. Furthermore, the adiabatic temperature estimation method also showed that heat transfer was very important and that a plug flow assumption over the entire melting zone was not correct. More research is needed to explain these differences.

Principal Components Analysis was demonstrated to be a valuable tool to quantify the effects of Q, N, barrel temperature and screw geometry on steady state, pulse and RTD data. PCA showed that there is a statistically valid correlation between the independent variables and measured time and energy input quantities.

Initial results from powder extrusion pulse tests showed a significant difference between pellet and powder power responses. The pulse test was used to show differences in melting kinetics for small changes in screw design. The results of this work demonstrate the power of this novel dynamic perturbation method as a tool to gain new insights into the melting process. Part II [4] advances the concept of energy input and loss.

## Nomenclature

Q/N, TBBL = Rate/screw speed, barrel temperature  
 $t_{\text{Delay}}$ ,  $t_{95\%}$  = Minimum and 95% residence times  
 $t_{\text{Mean}}$ ,  $t_{\text{Avg}}$  = Mean residence time  
 $t_{\text{Export}}$ ,  $t_{\text{Peak}}$  = Pulse power transport and peak times  
 $t_{M\ 1/2}$  = Melting half time (at 50%  $\text{SpE}_{\text{Pulse}}$ )  
 $P(t)$ ,  $E(t)$  = Power and energy input  
 $\text{SpE}_{\text{Pulse}} = \text{SpE}_{\text{Plug}} + \text{SpE}_{\text{Fluid}}$ , Pulse specific energies  
 $\text{NDM} = t_{M\ 1/2} / t_{\text{Mean}}$  modified Damkohler number

## References

- 1) M. D. Wetzel, D. A. Denelsbeck, S. L. Latimer, C.K. Shih, SPE ANTEC Tech. Papers, M3, 138, 2004.
- 2) M. D. Wetzel, D. A. Denelsbeck, S. L. Latimer, C.K. Shih, SPE ANTEC Tech. Papers, T18, 3791, 2003.
- 3) H. Chen, U. Sundararaj, K. Nandakumar, M. D. Wetzel, SPE ANTEC Tech. Papers, M3, 122, 2004.
- 4) M. D. Wetzel, D. A. Denelsbeck, S. L. Latimer, C.K. Shih, "Quantification of Melting Progression Part II," SPE ANTEC Tech. Papers, 2005.
- 5) C. G. Gogos, M. H. Kim, "Melting Phenomena and Mechanism in Polymer Processing Equipment", SPE ANTEC 2000.
- 6) M. D. Wetzel, "Experimental Study of LDPE Melting", SPE ANTEC Tech. Papers, 2002.
- 7) B.M. Wise, B.R. Kowalski, "Process Chemometrics in Process Analytical Chemistry," Blackie Academic & Professional, London, 1995, 259-312.
- 8) H. Potente, U. Melisch, Intern. Polymer Processing, XI (1996), 1, 29-41.
- 9) E. Gamache, P. G Lafleur, C. Peiti, B. Vergnes, Polymer Engg. & Science, 1999, 39(9), 1604-1613.
- 10) J. Brandrup, E. H. Immergut, Polymer Handbook, 3rd Edition, John Wiley, New York, 1989.
- 11) Z. Tadmor, C. G. Gogos, "Principles of Polymer Processing," John Wiley, New York, 1979, 264-273.

## Keywords

extrusion, melting, perturbation, pulse

| Polymer       | $V_{\text{Pellet}}$<br>(mm <sup>3</sup> ) | $\rho_{\text{Bulk}}$<br>(gm/l) | $\rho$<br>(g/cc) | $V_{\text{Solid}}$<br>(cc/l) | Friction<br>Coeff.<br>[8] | Friction<br>Coeff.<br>[9] | Friction<br>Coeff.<br>[10] |
|---------------|---|--------------------------------|------------------|------------------------------|---------------------------|---------------------------|----------------------------|
| Polypropylene | 45.3                                      | 573                            | 0.905            | 633                          | 0.25-0.4                  | 0.15                      | -                          |
| Polystyrene   | 32.6                                      | 614                            | 1.040            | 590                          | 0.2-0.7                   | -                         | 0.33                       |
| Polyethylene  | 32.2                                      | 627                            | 0.960            | 653                          | 0.1-0.25                  | 0.10                      | 0.20                       |

Table 1. Material Solid Properties

| Polymer       | $T_{\text{MP}}$<br>(°C) | $T_{\text{g}}$<br>(°C) | $\Delta H_{\text{f}}$<br>(J/gm) | $T_{\text{Onset}}$<br>(°C) | $\Delta H_{\text{Onset}}$<br>(J/gm) | $T_{\text{PT}}$<br>(°C) | $\Delta H_{\text{PT}}$<br>(J/gm) | $\Delta H_{200\text{C}}$<br>(J/gm) | $\lambda$<br>(W/m-K) | $\eta$ @67s <sup>-1</sup><br>200°C<br>(Pa.s) | $\eta$ @4300s <sup>-1</sup><br>200°C<br>(Pa.s) |
|---------------|-------------------------|------------------------|---------------------------------|----------------------------|-------------------------------------|-------------------------|----------------------------------|------------------------------------|----------------------|--|--|
| Polypropylene | 164                     | -                      | 143                             | 134                        | 162                                 | 172                     | 305                              | 352                                | 0.24                 | 805  | 54   |
| Polystyrene   | -                       | 104                    | -                               | 104                        | 95                                  | 150                     | 154                              | 210                                | 0.17                 | 1045   | 57   |
| HDPE MI 6.0   | 131                     | -                      | 213                             | 113                        | 150                                 | 137                     | 363                              | 443                                | 0.29                 | 860  | 86   |
| HDPE MI 18    | 130                     | -                      | 237                             | 112                        | 165                                 | 137                     | 402                              | 511                                | 0.29                 | 310  | 69   |

$\Delta H_{\text{On}} = \Delta H_{\text{PT}} - \Delta H_{\text{f}}$   $T_{\text{PT}}$  (phase transition complete)

Table 2. Material Thermal and Rheological Properties

| Polymer       | Steady State |              |                        |                       | RTD                      |                         |                          | Pulse Response           |                           |                         |                             |                  |                |                          |                 |  |                      |
|---------------|--------------|--------------|------------------------|-----------------------|--------------------------|-------------------------|--------------------------|--------------------------|---------------------------|-------------------------|-----------------------------|------------------|----------------|--------------------------|-----------------|--|----------------------|
|               | Power (J/s)  | Sp. E (J/gm) | T <sub>Melt</sub> (°C) | TC <sub>MZ</sub> (°C) | t <sub>Delay</sub> (sec) | t <sub>Mean</sub> (sec) | t <sub>Width</sub> (sec) | t <sub>xPort</sub> (sec) | P <sub>PEAK</sub> (J/s/g) | t <sub>PEAK</sub> (sec) | SpE@ <sub>PEAK</sub> (J/gm) | SpE Pulse (J/gm) | SpE VED (J/gm) | t <sub>M 1/2</sub> (sec) | N <sub>DM</sub> | T <sub>Ad</sub> @ <sub>PEAK</sub> (°C) | T <sub>Ad</sub> (°C) |
| Polypropylene | 1356         | 537          | 194                    | 186                   | 7.3                      | 14.9                    | 16.4                     | 4.4                      | 141                       | 5.9                     | 107.5                       | 389.0            | 281.5          | 6.5                      | 0.44            | 99.6                                   | 221                  |
| Polystyrene   | 1099         | 435          | 198                    | 192                   | 7.1                      | 19.9                    | 29.8                     | 3.5                      | 138                       | 5.2                     | 93.8                        | 244.0            | 150.2          | 5.4                      | 0.27            | 105.0                                  | 235                  |
| HDPE MI 6     | 1473         | 583          | 195                    | 168                   | 7.0                      | 15.0                    | 17.6                     | 4.4                      | 105                       | 6.0                     | 95.0                        | 340.0            | 245.0          | 6.8                      | 0.45            | 86.5                                   | 131                  |
| HDPE MI 18    | 1191         | 472          | 175                    | 162                   | 6.8                      | 14.6                    | 16.9                     | 4.4                      | 112                       | 6.0                     | 90.5                        | 350.0            | 259.5          | 6.9                      | 0.47            | 77.9                                   | 130                  |

Table 3. Material Response: Steady State, RTD and Pulse Response Data

| Screw Design | Steady State |              |                         |                         | RTD                    |                       |                          |                         | Pulse Data               |                        |                       |                           |                         |                             |                  |                  |                          |                 |                      |
|--------------|--------------|--------------|-------------------------|-------------------------|------------------------|-----------------------|--------------------------|-------------------------|--------------------------|------------------------|-----------------------|---------------------------|-------------------------|-----------------------------|------------------|------------------|--------------------------|-----------------|----------------------|
|              | Power (J/s)  | Sp. E (J/gm) | P <sub>LOSS</sub> (J/s) | SpE <sub>L</sub> (J/gm) | T <sub>Melt</sub> (°C) | TC <sub>MZ</sub> (°C) | t <sub>Delay</sub> (sec) | t <sub>Mean</sub> (sec) | t <sub>Width</sub> (sec) | t <sub>95%</sub> (sec) | t <sub>xP</sub> (sec) | P <sub>PEAK</sub> (J/s/g) | t <sub>PEAK</sub> (sec) | SpE@ <sub>PEAK</sub> (J/gm) | SpE Pulse (J/gm) | Sp. E VED (J/gm) | t <sub>M 1/2</sub> (sec) | N <sub>DM</sub> | T <sub>AD</sub> (°C) |
| 1            | 1356         | 537          | 354                     | 397                     | 194                    | 186                   | 7.3                      | 14.9                    | 16.4                     | 23.6                   | 4.4                   | 141.2                     | 5.9                     | 107.5                       | 389              | 282              | 6.5                      | 0.44            | 221                  |
| 2            | 1171         | 464          | 231                     | 372                     | -                      | 181                   | 6.7                      | 11.0                    | 8.2                      | 14.9                   | 3.8                   | 144.0                     | 6.1                     | 132.0                       | 349              | 217              | 6.5                      | 0.59            | 201                  |
| 3            | 1398         | 554          | 345                     | 417                     | 194                    | 186                   | 8.8                      | 14.5                    | 11.5                     | 20.2                   | 3.6                   | 152.0                     | 5.8                     | 128.7                       | 428              | 299              | 6.4                      | 0.44            | 245                  |

Table 4. Screw Design Response @9.1kg/hr and 200RPM: Steady State, RTD and Pulse Response Data

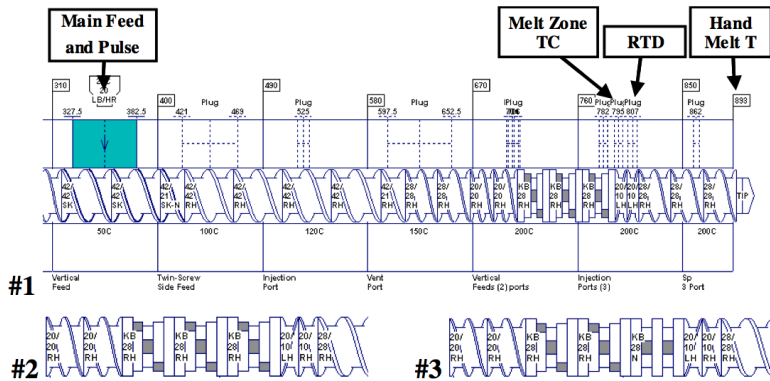


Figure 1. Open-discharge Experimental Setup showing Screw #1, and Screws 2 and 3

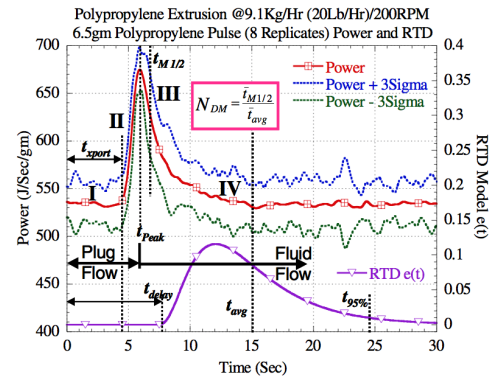


Figure 2. PP Extrusion, PP Pulse and RTD Response

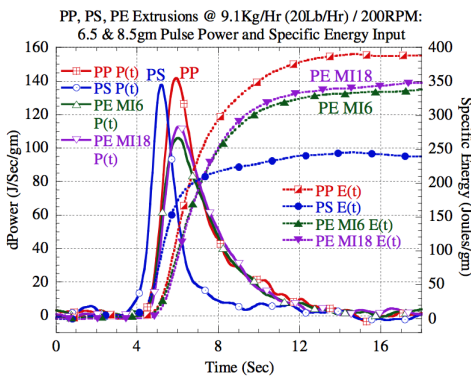


Figure 3. Pulse Power and Specific Energy for 4 Materials

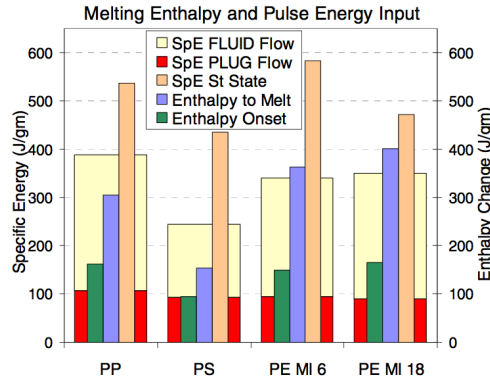


Figure 4. Energy Input and Melting Enthalpy

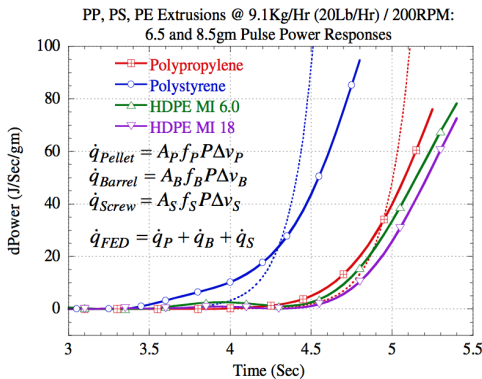


Figure 5. Frictional Energy Input from Pulse Response

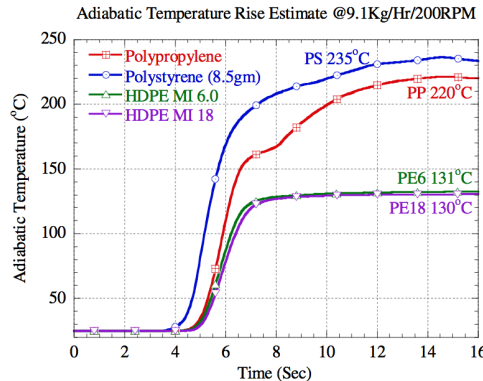


Figure 6. Adiabatic Temperature Rise Estimate

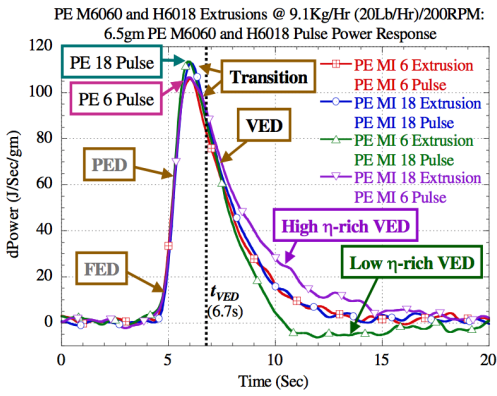


Figure 7. Molecular Weight Effect: Pulse Power

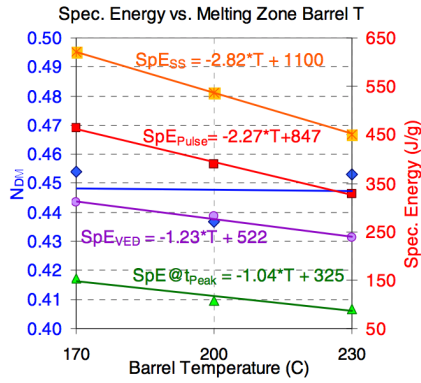


Figure 8. Barrel Temperature Effect: PP Energy Input

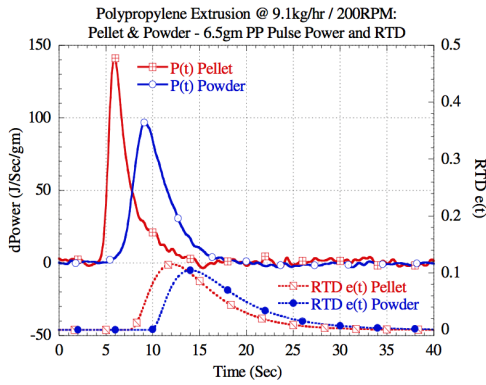


Figure 9. Effect of Material Form: Powder Pulse Response

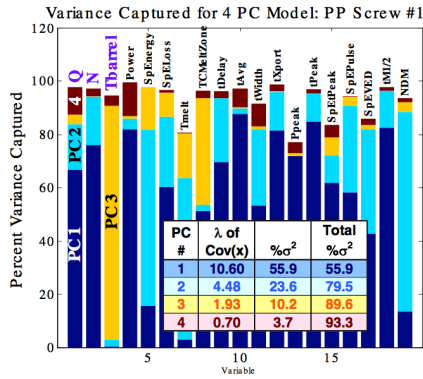


Figure 10. PP Extrusion, PCA Contribution Plot

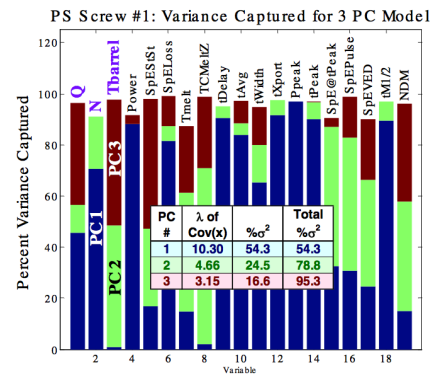


Figure 11. PS Extrusion, PCA Contribution Plot

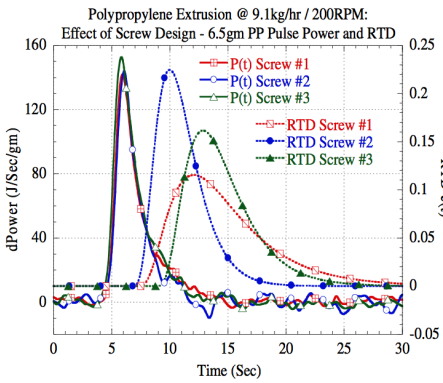


Figure 12. Screw Design, Pulse Power and RTD

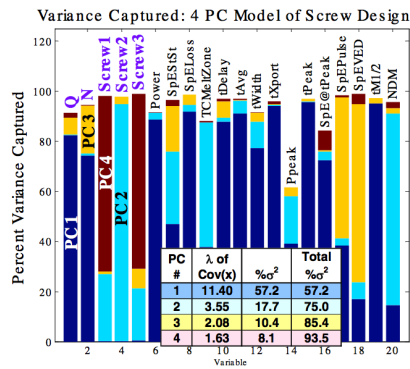


Figure 13. Screw Design, PCA Contribution Plot

Return to [Best Papers](#).